Iranian Journal of Geophysics, Vol 16 No 4, 2023, Page 53 – 68 (Research Article)
DOI: 10.30499/ijg.2022.314034.1377

Evidence of active faulting in the Azarshahr-Tabriz fault zone of northwestern Iran

Saeid Rahimzadeh [1], Noorbakhsh Mirzaei[2*] and Yasamin Moshasha[3]

[1] *Ph.D. student, Department of Seismology, Institute of Geophysics, University of Tehran, Tehran, Iran*
[2] *Professor, Department of Seismology, Institute of Geophysics, University of Tehran, Tehran, Iran*
[3] *M.Sc., Department of Seismology, Institute of Geophysics, University of Tehran, Tehran, Iran*

(Received: 8 November 2021, Accepted: 30 April 2022)

Abstract

The 1641 Dehkhwargan-Tabriz earthquake (Ms 6.8) is the only destructive earthquake to have occurred in Azarshahr-Khosrowshahr-Osku region of northwestern Iran. Ambiguities regarding the causative fault of this earthquake were a motivation to someway declare its mechanism. In this study, by conducting a field survey in an area between Tabriz and Azarshahr, and use of satellite imagery and aerial photographs, we provide geologic and geomorphic indications to identify the poorly known Azarshahr-Tabriz fault zone (ATF), which passes through the meizoseismal region of the 1641 earthquake. Our observations highlight the presence of a sinistral active fault zone that extends ~40 km in length from south of Tabriz to the northeast and north of Azarshahr to the southwest. The ATF is a structural assemblage of several fault strands with a variety of extensional and compressional mesoscale structures. We estimated slip rates ranging from ~0.01 mm yr−1 to <1 mm yr−1, based on drainage offset measurements, which demonstrate a relatively stable tectonic environment located immediately south of the well-known seismically active dextral North Tabriz fault.

Keywords: Azarshahr-Tabriz fault zone, Northwestern Iran, Osku, seismogenic fault, seismic hazard, transtension structure

*Corresponding author: nmirzaii@ut.ac.ir

1 Introduction

The knowledge of the seismogenic faults in seismic regions is critical to understand their seismic hazard. Since the mid-20th century, the study of active faults as potential sources of earthquakes, ground deformation, and understanding recent and contemporary tectonogenesis have become the special object of research (Trifonov and Kozhurin, 2010). The Turkish-Iranian plateau represents a complex collision boundary zone between the converging Arabian and Eurasian plates. The continental shortening in this region, is accomplished by both thickening and lateral expulsion of continental crust in the collision zone (e.g., De Mets et al., 1990; Jackson, 1992).

Conspicuous right-lateral strike-slip faulting in NW Iran along the North Tabriz fault (NTF), the Gailatu-Siah Cheshmeh-Khoy (GSK) fault, and the Chalderan fault, continues to eastern Turkey along the North Anatolian fault (NAF) (e.g., Khorrami et al., 2019). The subject of this paper is the Azarshahr-Tabriz region immediately south of the NTF, which covers a part of the northwestern-most region of Central Iran (Figure. 1). Central Iran is commonly interpreted as a former microcontinent and behaves more or less as a rigid block in the overall compressive regime because of Arabia-Eurasia convergence (e.g., Berberian, 1981, 2014; Mirzaei et al., 1998). The target region consists of a poorly-known left-lateral strike-slip fault zone, passing through meizoseismal area of the 1641 Dehkhwargan-Tabriz historic earthquake, a conjugate to the well-known seismically active NTF system.

The aim of this paper is not to present details of structural geology and active tectonics of the Azarshahr-Tabriz region, but (1) to introduce field indications for a poorly-known or even unknown active fault zone responsible for the 1641 Dehkhwargan-Tabriz historic earthquake, and (2) to give an overview of the geometry and kinematics of structures in the Azarshahr-Tabriz fault zone (ATF). Data and interpretations are mainly derived from field observations and satellite images.

The study region is covered by Pliocene-Quaternary alluviums, terraces, plane deposits, gravel fans, volcanic block deposits, and mainly andesitic rocks that make young Sahand volcanic domes (See Figure. 2 for a geological map of the target region). No detailed studies on active deformation have been performed on the areas south of the NTF as the most important seismogenic structure in northwestern Iran (see Figures. 1 and 2); therefore, there is insufficient information about the kinematics of active deformation of the study region. Recently, Taghipour et al. (2018) studied geological indications along the Salmas and Maragheh fault zones in the west of our target area. Here, we use satellite imagery, aerial photographs, and field observations to provide geological indications of a sinistral active fault zone in an area between Tabriz and Azarshahr (Figure. 1), where a historic earthquake with an estimated surface-wave magnitude (Ms) of 6.8 struck Dehkhwargan (modern Azarshahr), Osku and Khosrowshah (modern Khosrowshahr) regions in 1641.

2 Tectonic setting

Iran is a wide compressional deformation and seismic activity zone along the Alpine-Himalayan mountain belt, entrapped between the stable Arabian and Eurasian plates. Most of the territory is characterized by continental collision accommodated by fold- and thrust mountain ranges of the Zagros (in the west and southwest), Alborz (in the north), Kopeh Dagh (in the northeast); and subduction takes place in the Makran region of southeastern Iran and southern Pakistan (e.g., Mirzaei et al., 1998; Berberian, 2014; Khorrami et al., 2019). The geological structures and

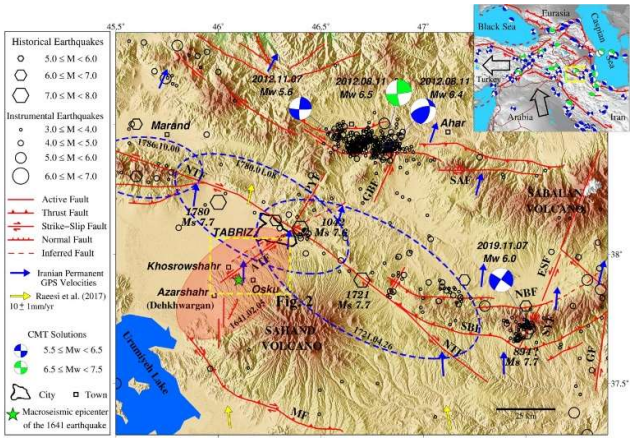

Figure1. Simplified seismotectonic map of Tabriz and nearby regions. Focal mechanism solutions of large (Mw ≥ 5.5) earthquakes are presented. Iranian permanent GPS velocity vectors are taken from Khorrami et al. (2019). The green star represents the macroseismic epicenter of the 1641 Dehkhwargan-Tabriz earthquake as proposed by Ambraseys and Melville (1982). NTF: North Tabriz Fault; ATF: Azarshahr-Tabriz Fault; MF: Maragheh Fault; NBF: North Bozqush Fault; SBF: South Bozqush Fault; SYF: Shalgun-Yelimsi Fault; SAF: South Ahar Fault; PYF: Payan Fault, ESF: East Sarab Fault; Gf: Garmachay Fault; GBF: Guyjabel Fault. Major faults are mainly based on Solaymani Azad et al. (2019). Our study area is outlined by the yellow rectangle. A simplified active fault map of northwestern Iran, eastern Turkey, and Caucasus is shown in the inset (redrawn and updated after Jackson (1992)).

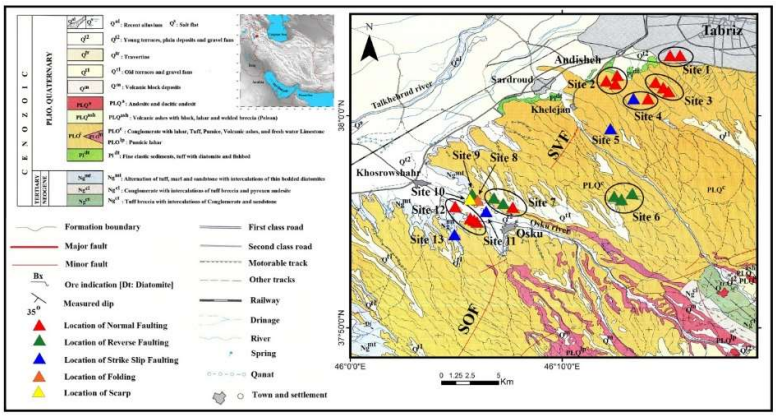

Figure2. Geological map of Osku and adjacent regions. This map is compiled from the 1:100000 Osku and a part of Tabriz geological maps from Khodabandeh and Amini Fazel (1993) and Asadian (1993), respectively; published by the geological survey of Iran. Triangles are observation sites in the field survey. SVF: South Varanag Fault: SOF: South Osku Fault.

seismicity of northwestern Iran are attributed to continental collisions after the closure of the Neo-Tethys Ocean in the middle-late Eocene (Hempton, 1987; Vincent et al., 2005) or late Miocene (Berberian and Berberian, 1981; Dewey et al., 1986; McQuarrie et al., 2003), with a late Miocene timing being supported by the onset of crustal uplift (Gavillot et al., 2010; Mouthereau, 2011; Bottrill et al., 2012; Ghalamghash et al., 2019).

The tectonic activity of northwestern Iran, is due both to the northward convergence of Central Iran toward Eurasia and to the eastward motion of the Lesser Caucasus area towards the NNE concerning Eurasia, inducing distributed conjugate strike-slip faulting and related basin formations (Ritz et al., 2006; Gurbuz and Saroglu, 2018). The most conspicuous

earthquake fault in northwestern Iran is the dextral NTF (Figure. 1), which has an estimated slip rate of 7–8 mm/year (Rizza et al., 2013; Allen, 2020). These structures continue to the Turkey and Armenia and have been interpreted by Copley and Jackson (2006) as an array that rotates anticlockwise, permitting greater plate convergence in the east than to the west, consistent with the GPS-based strain measurements (Reilinger et al., 2006; Allen, 2020).

In northwestern Iran, the Caucasus, and eastern Turkey, the strain is partitioned to almost pure reverse faulting across the northern Kura Basin, and the southern Greater Caucasus in Azerbaijan, presumably on the Main Caucasus thrust fault (MCTF), and right-lateral strike-slip along the NTF, the Gailatu-Siah Cheshmeh-Khoy (GSK) fault, the Chalderan fault, and continuing along the North Anatolian fault (NAF) in Turkey (Khorrami et al., 2019). Because of this partitioning, Turkey moves westward relative to Eurasia, as a wedge between North Anatolian and East Anatolian conjugate strike-slip faults (see inset in Figure. 1), while the Lesser Caucasus and northwestern Iran show an easterly component of motion relative to Eurasia (e. g., McKenzie, 1972; Jackson and McKenzie, 1984; Jackson, 1992). This has induced E-W compression between the Talesh and the South Caspian Basin, consistent with the fault plane solutions of earthquakes and overall seismicity of the N-S faults extending from the Alborz to the Kura basin along the Caspian shoreline (Jackson et al., 2002). The existing focal mechanism solutions of earthquakes (e.g., GCMT solutions (www.globalcmt.org, last accessed 1 February 2021) confirm the present-day dominance of strike-slip motion in the region (see inset in Figure. 1). Sinistral NNE-SSW striking faults of northwestern Iran are known as active conjugates to the NW-SE major dextral ones (e.g., Berberian, 2014; Faridi et al., 2017).

The main active fault system of northwestern Iran is NTF, with conspicuous history of seismicity (Ambraseys and Melville, 1982; Berberian, 2014) that plays a controlling role in the geodynamics of the region (Solaymani Azad et al., 2019). It is one of the boundary structures between Azarbayejan-Alborz and Central-East Iran major seismotectonic provinces (see Figure. 4 in Mirzaei et al., 1998). From seismotectonic point of view, the study region in this paper is a part of Central Iran seismotectonic subprovince which is a low strain rate intraplate environment located in the area south of the NTF. We suppose that a sinistral fault with a trend orthogonal to the well-documented NW–SE striking dextral NTF passes through the meizoseismal area of the 1641 Dehkhwargan-Tabriz earthquake.

3 Seismic history of northwestern Iran

Northwestern Iran has witnessed large historical earthquakes of 1042 (*Ms 7.6*), 1273 (*Ms 6.5*), 1721 (*Ms 7.7*), 1780 (*Ms 7.7*) in Tabriz; 1641 Dehkhwargan-Tabriz (*Ms 6.8*); 1304 (*Ms 6.7*), and 1786 (*Ms 6.3*) in Marand (Ambraseys and Melville, 1982; Figure. 1). The NTF that cuts through Tabriz, one of the largest cities of Iran with a population of about 1.5 million, and adjacent reverse faults ruptured from southeast to northwest in a cluster of three large historical earthquakes in 65 yr (see Figure. 1 for meizoseismal areas of these events): the Shebli earthquake in 1721 on the southeastern segment, the Tabriz earthquake in 1780 on the northwestern segment and the Marand-Mishu earthquake in 1786 on the Mishu reverse fault and the Sufian segment of the NTF (Figure. 1; Berberian, 1997; Berberian and Yeats, 1999). Because of these three historical earthquakes, more than 240000 people were killed (Ambraseys and Melville, 1982). In contrast to the historical seismicity, the

most conspicuous and destructive earthquakes in the instrumental time period that shook up northwestern Iran are Ahar-Varzegan twin earthquakes with a short time difference of 11 minutes on 11 August 2012, M_w *6.4* (M_w 6.5 GCMT) at 12:23 UTC and M_w *6.3* (M_w 6.4 GCMT) at 12:34 UTC, and epicenters distance of about 6 km (Figure. 1), occurred on an east-west striking fault zone north of the NTF (e.g., Copley et al., 2014; Yazdi et al., 2018). These earthquakes killed over 300 people and injured over 3000 (Copley et al., 2014). The most recent large earthquakes in this area are Turkmanchai earthquake on 07 November 2019, M_w 6.0, and Qotor earthquake on 23 February 2020, *Mw* 6.0 (Figure. 1). The epicenter of the 2019 Turkmanchai earthquake was located ~110 km southeast of Tabriz, in a tectonically complex fold-and-thrust mountain range and killed at least five people, injured hundreds and widespread damage to the surrounding villages (Valerio et al., 2020). The February 2020 Qotor earthquake occurred at ~170 km northwest of Tabriz near the Iran-Turkey border; it killed at least 10 people and injured over 100 as mentioned in the news.

3.1 The 1641 Dehkhwargan-Tabriz earthquake

On February 5th 1641, in a region south of Tabriz and East of Lake Urumiyeh, an earthquake with an estimated surface-wave magnitude (Ms) of 6.8 struck Dehkhwargan (modern Azarshahr), Osku, and Khosrowshah (modern Khosrowshahr) regions; and many public buildings, including historical monuments, collapsed in Tabriz (Ambraseys and Melville, 1982; Figure. 1). The macroseismic epicentre for this earthquake was located south of Tabriz, but the meizoseismal area does not correspond to any mapped fault (Berberian and Yeats, 1999; Rizza et al., 2013). This is the only damaging earthquake recorded in the Azarshahr, Khosrowshahr, and Osku regions of East Azarbaijan province, along the northwestern foothills of the Sahand volcano. Because of this earthquake, Osku and Khosrowshah, on the northwest slopes of Mount Sahand, as well as Dehkhwargan, were totally destroyed and caused 1200 fatalities and considerable damages in the epicentral region and nearby areas (Melville, 1981). The meizoseismal area of this earthquake, as defined by Ambraseys and Melville (1982), shows an ellipse shape region (see 0. 1), located in the northwestern flank of the Sahand volcano, with a long axis of ~40 km, trending NE-SW, approximately parallel to the Talkhehrud River (see Figure. 2 for the position of Talkhehrud; rud is a Persian word that means river). Despite large-scale rockfalls in the mountains, no evidence for ground deformations of tectonic origin was found (Berberian and Yeats, 1999).

In the next section, we will describe the geological and morphotectonic evidence for an active fault zone passing through the meizoseismal area of the 1641 Dehkhwargan-Tabriz earthquake which appears to have been the causative fault of this event.

3.2 The causative fault of the 1641 earthquake in the literature

Berberian (1997) and Berberian and Yeats (1999) pointed out that the northeast-trending meizoseismal area of the 1641 Dehkhwargan-Tabriz earthquake does not correspond to any mapped fault or surface lineament in the aerial photographs. According to Berberian (2014), the causative fault of the 1641 earthquake is not known. Based on the meizoseismal area of the earthquake, he has stated that the 1641 earthquake, might have occurred on a line along the Talkhehrud fault (an inferred fault along the Talkhehrud River; see Figure. 2). Berberian (2014), also, has suggested three possibilities for the Talkhehrud fault: “(i) a

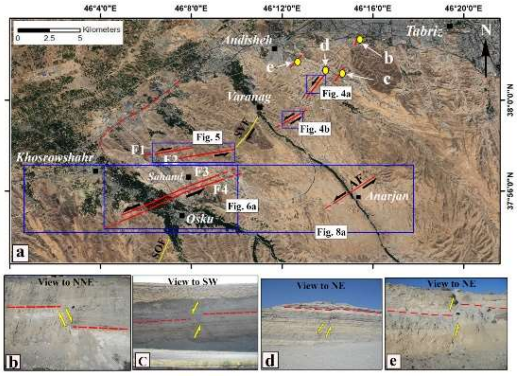

Figure3. (a) Google Earth satellite imagery of the Azarshahr-Tabriz fault zone. Blue quadrangles indicate the sites with observed left-lateral strike-slip displacement. Circles filled with yellow color show the locations of normal faults. The yellow lines depict the active faults from the geological map of Osku (scale 1:100000). SOF: South Osku Fault; SVF: South Varanag Fault; AF: Anarjan Fault. (b-e) Field photographs of normal faults (see also sites 1-4 in Figure. 2).

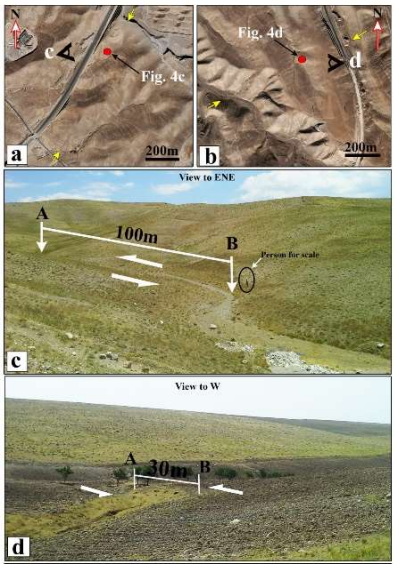

Figure4. (a and b) Left-lateral river-offset (sites 4 and 5 in Figure. 2, respectively; marked as rectangles in Figure. 3a). Yellow arrows represent the fault trace. The 'eye' symbols in a and b show the approximate viewpoint. (c) ENE view of an about 100 m left-lateral drainage offset (A-B) in the southeast of Andisheh suburb (site 4 in Figure. 2; see Figure. 4a for the location on satellite imagery). (d) Westward view of an about 30 m left-lateral drainage offset (A-B) in the southeast of Khelejan village (site 5 in Figure. 2; see Figure. 4b for the location on satellite imagery).

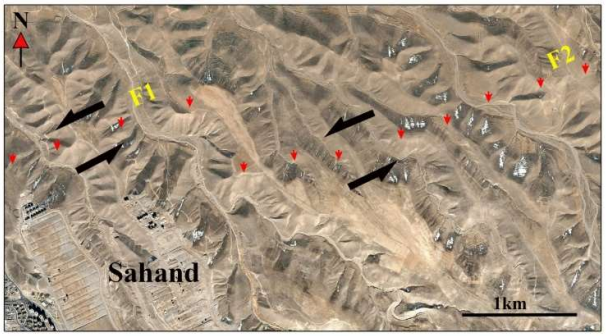

Figure5. Right-stepping fault segments and left-lateral deflection of the drainage pattern in the north of the town of Sahand. Red pointers represent the fault segments traces. See also Figure. 3a for the location.

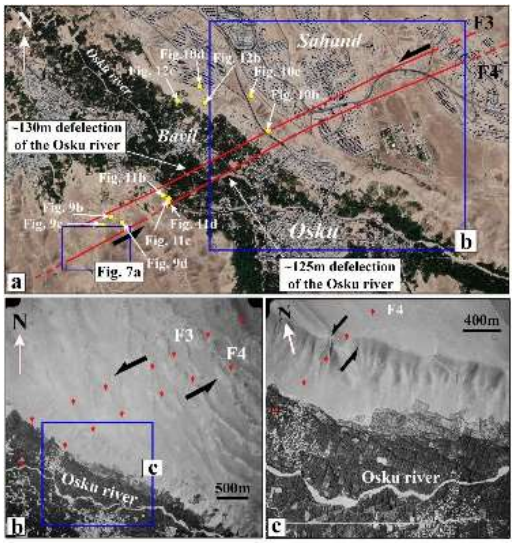

Figure 6. (a) Google Earth satellite imagery, showing left-lateral deflection of the Osku River (site 11 in Figure. 2). See also Figure. 3a for the location. Yellow circles show the locations of surface faulting photos. (b and c) Aerial photographs (February 1967) showing left-lateral deflection of the drainage pattern, north of Osku. Red pointers represent the fault segments traces.

NNE–SSW-tending cross blind thrust (similar to the 1968 Dasht-e Bayaz and Ferdows sequence; Berberian, 1981; Berberian and Yeats, 1999); (ii) a conjugate strike-slip fault to the North Tabriz fault (similar to the 1986 North Palm Spring and the 1992 Joshua Tree, … earthquakes; Yeats, 2012; the South Rigan earthquakes of 20 December 2010 and 27 January 2011; Walker et al., 2013); or (iii) a normal fault responsible for the formation of the Tabriz plain as a pull-apart basin covered by the Sahand volcanic lava and ash". Faridi et al. (2017) introduced the Dehkhwargan fault in brief and stated that it exceeds 20 km in length on aerial photos and satellite images and deflects left laterally the drainage pattern to the north of Azarshahr (see Figures. 1b and 9 in Faridi et al., 2017). They also pointed to the westward flowing rivers that radiate from the Sahand volcano and show, in some cases, 200 m left-lateral offset at their intersection with the Dehkhwargan fault. According to Faridi et al. (2017) distortion of cover, volcanoclastic rock units along Dehkhwargan fault demonstrate that it is an active basement structure beneath the Sahand volcano. Solaymani Azad et al. (2019) in their work on active tectonics and geodynamics of northwestern Iran point to dextral NNW-striking faults within the Azarshahr-Mamaghan and Osku regions (see Figure. 6 in Solaymani Azad et al., 2019), where the 1641 Dehkhwargan earthquake, occurred.

It is noteworthy that Faridi et al. (2017) introduced Dehkhwargan fault as a sinistral fault based on an aerial photograph and drainage pattern, but Solaymani Azad et al. (2019) have assertions on the contrary and introduce the same fault zone as a dextral fault based on a drainage deflection.

4 Geologic and geomorphic evidence

The diversity of proposed characteristics and possible models for the causative fault of the 1641 Dehkhwargan-Tabriz earthquake, as introduced in section 3.2, demonstrated the necessity of field survey to somehow declare ambiguities regarding the mechanism of the causative fault, based on reliable geological and morphotectonic evidence. Here, we knew the meizoseismal region from damage reports of the 1641 earthquake (Figure. 1)

and this helped in delimiting the area where to start field investigations.

The region between Azarshahr and Tabriz, where the meizoseismal area of the 1641 earthquake was situated, is covered by the Pliocene-Quaternary sediments and volcanic deposits. In this area, extensional landforms are abundant as can be expected in a volcanic region. Indications of left-lateral strike-slip deformations can be observed in aerial photos and satellite images of the study area. We visited thirteen observational sites (see Figure. 2) to document deformations. In sites 1 to 3, in the northeastern part of the target fault zone, near Tabriz, just a number of normal faults were observed. About 4 km southwest of Tabriz, where normal faults still prevail (site 4 in Figure. 2; Figure. 3) left-lateral drainage offset with horizontal displacement of about 100 m was observed (Figures. 4a and c). Further southwest, we observed another clear left-lateral strike-slip offset with horizontal displacement of about 30 m (site 5 in Figure. 2; Figures. 4b and d). The ages of the drainage offsets are not known, but since both drainages incised within the middle Pleistocene (maximum 780 ka; Khodabandeh and Amini Fazel, 1993; Asadian,1993; Figure. 2) sediments, we approximate a slip rate of <1 mm yr^{-1} and <<1 mm yr^{-1} for the first offset and the second offset, respectively; which seems feasible for an intraplate setting.

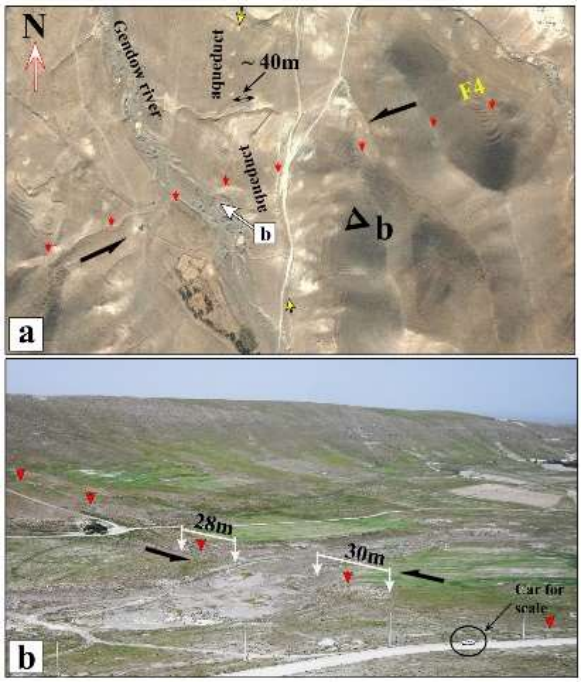

Figure 7. (a) Google Earth satellite imagery showing left-lateral deflection of the Gendow River (site 13 in Figure. 2), and aqueduct offset (most likely not related to faulting). Red pointers represent the fault segment trace. The 'eye' symbol in (a) shows the approximate viewpoint. See also Figure. 6a for the location. (b) WNW view of 28-30m Left-lateral strike slip offset along Gendow River (site 13 in Figure. 2).

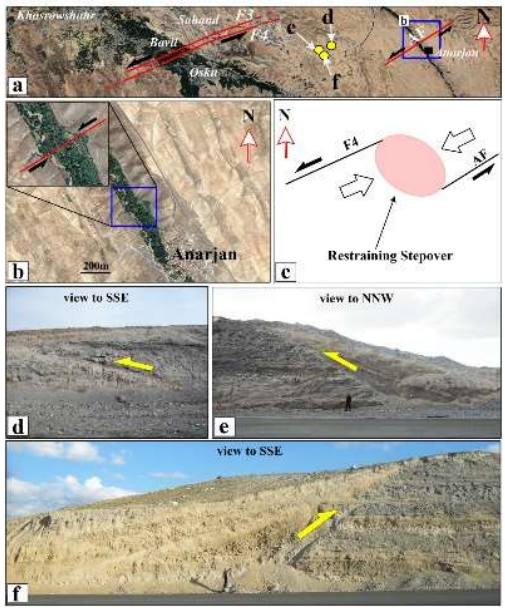

Figure 8. (a) Google Earth satellite imagery of a part of the Azarshahr-Tabriz fault zone. Yellow circles show the locations of surface faulting photos. (b) Google Earth satellite imagery of the Anarjan, showing left-lateral deflection. (c) Formation mechanism of the restraining stepover, between F4 and Anarjan Fault segments of the Azarshahr-Tabriz sinistral fault system. (d-f) Field photographs of NNW striking reverse faults within the restraining stepover, between F4 and Anarjan Fault (site 6 in Figure. 2).

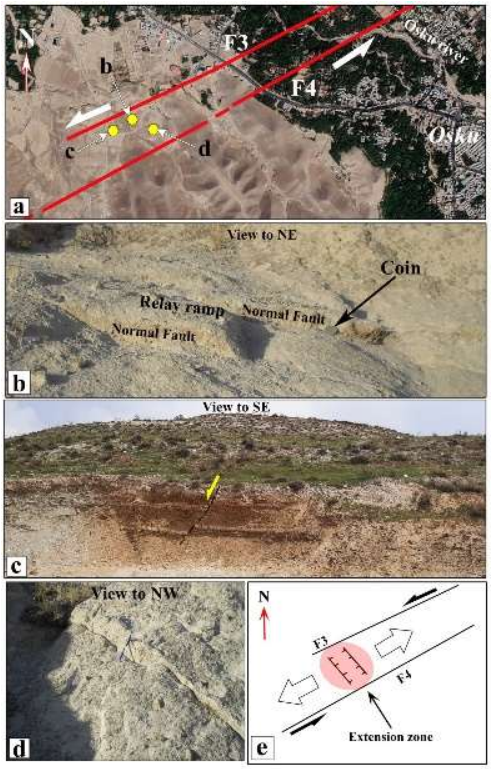

Figure 9. (a) Local extension zone between F3 and F4 left-stepping fault segments along the through going Azarshahr-Tabriz fault zone (site 12 in Figure. 2). Yellow circles show the locations of surface faulting photos. (b-c) extensional structures in between F3 and F4 segments. (e) Formation mechanism of the extension zone, between F3 and F4 segmens.

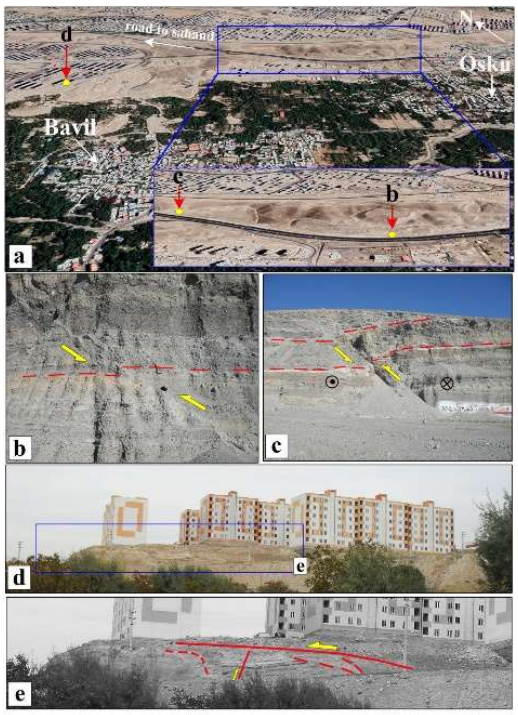

Figure 10. (a) Google Earth satellite 3D image of the Osku region. The inset shows the locations (yellow circles) of the depicted reverse faults in (b) and (c); both exposed in a cut slope approximately perpendicular to the Azarshahr-Tabriz fault zone, nearby Osku (site 7 in Figure. 2). (d and e) Photo of a very low angle reverse fault dipping ENE in ~1.5 km north of Bavil village, and its interpretation (site 9 in Figure. 2).

North of the town of Sahand, two ENE striking sinistral fault segments, we call them F1 and F2, that incised the Middle Pleistocene old terraces and gravel fans, runs parallel with a right stepping arrangement (Figure. 5); and two other parallel NE-SW sinistral faults, F3 and F4, pass through the town and to the southwest deflect the Osku River left-laterally with displacements of about 130 and 125m, respectively (Figure. 6a). The age of the river channel is not known, but since the both incised surfaces are within the Upper Pleistocene (maximum 125 ka; Khodabandeh and Amini Fazel, 1993; Figure. 2) sediments, the slip rate will be ~1 mm yr^{-1}. Near the Dizaj village, southwestward of the deflection along the F4 (Figure. 7 and site 13 in Figure. 2), one more left-lateral drainage offset with a horizontal slip of 28-30 m (Figure. 7b) is visible. Based on the incised presumed Upper Neogene (maximum 2500 ka; Khodabandeh and Amini Fazel, 1993; Figure. 2) sediments, the approximate slip rate is ~0.01 mm yr^{-1}.

Another left-lateral drainage offset with horizontal displacement of 50-60 m (Figures. 8a and b) along a NE striking fault trace, in the southeast of F4, is visible on Google Earth satellite image; we call it Anarjan fault. The morphology of the Northeast and southwest of the Anarjan has been reworked by human activities and there is no preserved geomorphic evidence for the continuation of the fault trace. F4 and Anarjan fault make a right-stepping restraining stepover, within which relatively low-angle reverse faults with opposite dip directions have been exposed (Figure. 8).

Near to Osku, F3 and F4, as a couple of parallel sinistral fault segments, make a local extensional environment, in which a relay ramp structure associated with normal faulting in the volcanic ashes has developed (Figure. 9). This feature can be key field evidence and a clue to the definition of seismogenic normal faulting (see Bucci et al., 2006) along the throughgoing Azarshahr -Tabriz sinistral fault zone. Northwest of Osku, where a road to the new-town of Sahand is under construction; in an NW-SE section (Figure. 10), an assemblage of exposed reverse faults offset the topography in nearly vertical cut slopes, among them some show a left-lateral strike-slip component. On the southeastern block of the F3, a set of normal faults has formed (Figure. 11 and site 12 in Figure. 2). The location of reverse faults and normal faults is consistent with strike-slip tectonics.

In a site west of Osku, a typical negative flower structure (Figure. 11d) is visible in a profile perpendicular to the strike of the fault zone that implying a transtensional stress field. Near to this structure, there exist plenty of normal faults close to each other (e.g., Figures. 11b and c). North of Bavil village, in a nearly vertical cut slope, an interesting fault-related Z-shaped fold is visible, which is a key structure for kinematic interpretation (Figure. 12b). About 400 m to the west of this site, there exists a small scarp with a vertical displacement of about 160 cm (Figure. 12c). From the morphology of this feature and its surrounding, we could not assure that it is a fault scarp or remnant of a landslide. If possible, this scarp is a remnant of a fault scarp produced by the historic/prehistoric earthquakes that occurred in this region, then it is a valuable reference point for paleoseismological studies.

Historical aqueducts, built in the southeast-northwest direction, are one of the remarkable manmade structures of the Osku region that provide a major proportion of the agricultural water in the region. A seeming incised aqueduct (we call it the Gendow aqueduct) shows a left-lateral offset of ~40 m approximately parallel to F4 on a satellite image (Figure. 7a). If we relate this offset to a fault strand parallel to F4 and assume a very approximate age of 3000 years for Gen-

dow aqueduct, which is likely to be a maximum age for the construction of aqueducts in northwestern Iran (Forbes, 1964; Goblot, 1979; Kamiar, 1983; Potts, 1990; Hessami et al., 2003), the slip-rate will be ~13 mm yr^{-1}. Although not impossible, this seems too high, given the estimates derived from the river channel and offset drainages described above. Therefore, it is most likely that the aqueduct offset is not a reliable marker of the fault displacement and slip measurements in this region. As discussed by Allen et al. (2011), for the same phenomenon in the Zarand region of southeastern Iran, the aqueduct may not have originally been a linear feature built across the fault, for example.

4.1 Azarshahr-Tabriz fault zone

Meizoseismal area of the 1641 Dehkhwargan-Tabriz earthquake (Ambraseys and Melville, 1982), coincides well with the deformations and landforms we observed in the field (section 4). Our observations highlight the presence of an active fault zone that extends ~40 km in length from south of Tabriz to the northeast and north of Azarshahr to the southwest (Figure. 1). The fault zone cuts through poorly cemented conglomerates with lahar, Tuffs, Pumice, volcanic ashes, and freshwater Limestones of Pliocene-Quaternary age (Figure. 2). The fault zone consists of a structural assemblage of at least ten fault strands with a variety of extensional and compressional mesoscale structures and their associated morphotectonic landforms. Only two out of ten fault strands have been previously demonstrated on the geological maps (scale 1:100000) of the region published by the Geological Survey of Iran.

Observed structures and topographic offsets in the field, as well as landforms and deflected features on satellite images and aerial photos of the region, as introduced in section 4, demonstrate a sinistral fault zone with a normal dip-slip component that we call ATF. N to NNE directed Global Positioning System (GPS) velocity vectors (Khorrami et al., 2019) in the study region (see Figure. 1), also, supports the left-lateral strike-slip mechanism of the fault zone.

The concentration of earthquakes, recorded by the northwestern Iran seismographic network (a subnetwork of the Iranian Seismological Center: http://irsc.ut.ac.ir), and macroseismic epicenters of major historical earthquakes (Figure. 1), may imply that the ATF intersects (or terminates at) the NTF to the north.

5 Discussion

From the published scientific documents it is clear that there is a serious ambiguity regarding the causative fault of the 1641 Dehkhwargan- Tabriz earthquake. A line along the Talkhehrud fault has been proposed by Berberian (2014) as a possible source of this earthquake. Faridi et al. (2017), proposed an active NE-SW striking sinistral basement structure beneath the Sahand volcano passing through the meizoseismal area of the 1641 Dehkhwargan-Tabriz earthquake; and Solaymani Azad et al. (2019) pointed to dextral NNW-striking faults within the region, where the 1641 Dehkhwargan earthquake, occurred. To overcome this problem, we conducted fieldwork and review of available written documents as well as air photos and satellite imageries.

Recognition of at least ten fault strands with a variety of extensional and compressional mesoscale structures as well as horizontal left-lateral displacements of up to 130 m, in our field survey, as introduced in section 4, altogether, confirms a NE striking sinistral fault system that extends in the area between Azarshahr and Tabriz and passes through the meizoseismal region of the 1641 Dehkhwargan-Tabriz earthquake. The strike-parallel components of the measured GPS velocity vectors (Khorrami et

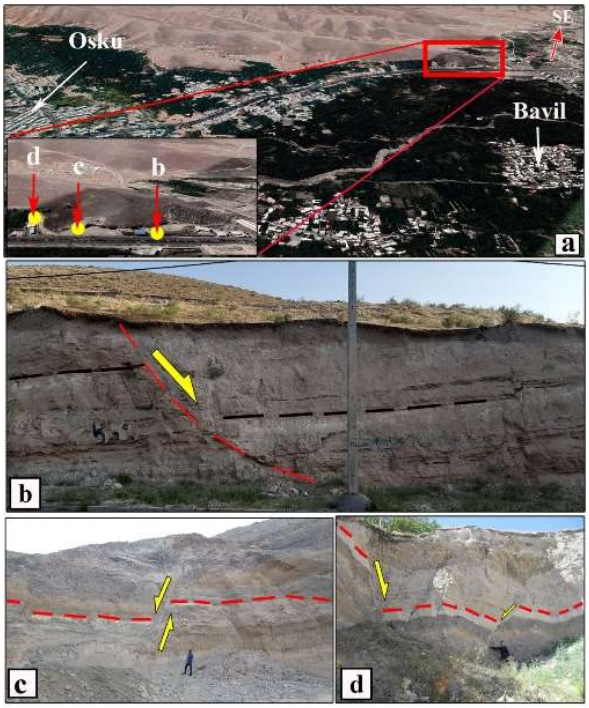

Figure 11. (a) Google Earth satellite 3D image for the Osku region. The inset shows the locations of the exposed faults (yellow circles) depicted in b to e. (b-d) Photographs of extensional structures (normal faults (b and c) and negative flower structure (c)). Fault exposures (b to d) were observed in a trend approximately perpendicular to the Azarshahr-Tabriz fault zone, nearby Osku (site 12 in Figure. 2). Also, see Figure. 6a for the locations.

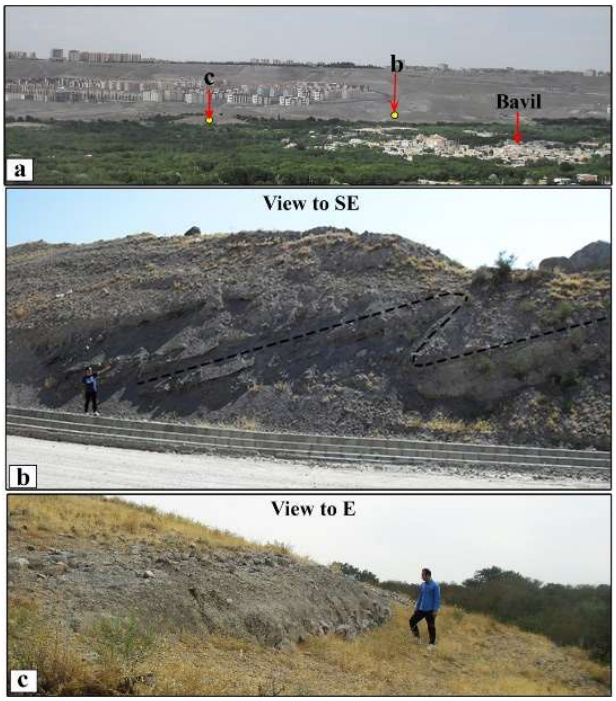

Figure 12. (a) NW view of Bavil village and its surrounding. Locations of a scarp and a Z-shaped fold in the north of the village are depicted by yellow circles in a and b, respectively. (b) and (c) Close view of the Z-shaped fold (site 8 in Figure. 2) and scarp (site 10 in Figure. 2), respectively. See also Figure. 6a for their locations.

al., 2019), also imply sinistral motion along with the ATF. In addition, the formation of a conspicuous Z-shaped fold formed along the fault zone,sinistral motion along with the ATF. In addition, the formation of a conspicuous Z-shaped fold formed along the fault zone, north of Bavil village, in a kinematic point of view indicates a sinistral basement fault; as discussed by Dooley and Schreurs (2012) via analog modeling of intraplate strike-slip tectonics.

From drainage offset measurements (Figures. 4c and d, 6a, and 7b), we estimated slip rates ranging from ~0.01 mm yr^{-1} to <1 mm yr^{-1}, which is consistent with the 0–3 mm yr^{-1} of possible extension normal to the NTF given by Djamour *et al.* (2011) and Rizza et al. (2013). Because the age of slip initiation controls the geologically derived slip rates, often the poorly constrained results may achieve. As an example, Talebian and Jackson (2002), calculated a slip rate of 10–17 mm yr^{-1} on the Main Recent Fault of Zagros assuming that the 50-km-long cumulated horizontal offset along the fault formed 3–5 Myr ago (Authemayou et al., 2009), that is at least two times higher than the velocity estimated using geodetic measurements, which give an upper bound of 5 mm yr^{-1} (Vernant et al., 2004; Vernant and Chery, 2006). Consistency between geodetically and long-term geologically derived slip rates may imply that geodetic data represent the long-term motion of this part of Iran. The estimated slip rates are compatible with a relatively stable intracontinental environment that its contribution to stress accommodation is small. So, the scarce seismicity in the Azarshahr-Khosrowshahr-Osku region could be related to such low strain rates which leads to very long return periods for large earthquakes.

The identification of poorly-known ATF which is responsible for the only documented large earthquake (Ms 6.8 in 1641) in Azarshahr-Khosrowshahr-Osku region, immediately south of the well-known seismically active dextral NTF system, has been the most important result of this work.

6 Conclusion

Diversity of proposed characteristics and possible models for the causative fault of the 1641 Dehkhwargan-Tabriz earthquake, demonstrated the necessity of field survey to somehow declare ambiguities regarding the mechanism of the causative fault, based on reliable geological and morphotectonic evidence. Recognition of at least ten fault strands with a variety of extensional and compressional mesoscale structures, in our field survey, confirms a NE striking sinistral fault system that extends ~40 km in the area between Azarshahr and Tabriz and passes through the meizoseismal region of the 1641 Dehkhwargan-Tabriz earthquake. From drainage offset measurements, we estimated slip rates ranging from ~0.01 mm yr^{-1} to <1 mm yr^{-1}, compatible with a relatively stable intracontinental environment that its contribution to stress accommodation is small. The scarce seismicity in Azarshahr-Khosrowshahr-Osku region could be related to such low strain rates which leads to very long return periods for large earthquakes. The interaction of the Azarshahr-Tabriz fault and North Tabriz fault could cause stress concentration at the junction. These are key issues in the determination of potential seismic sources for detailed earthquake hazard analyses and risk assessments, especially in the rapidly growing provincial capital city of Tabriz (population ~1.5 million).

References

Allen, M. B., Kheirkhah, M., Emami, M. H., Jones, S. J., 2011, Right-lateral shear across Iran and kinematic change in the Arabia-Eurasia collision zone. Geophys. J. Int. 184, 555–574.

Allen, M. B., 2020, Arabia-Eurasia Collision. In: Encyclopedia of Geology, 2nd edition, Elsevier Inc. 1-13, https://doi.org/10.1016/B978-0-12-409548-9.12522-9.

Ambraseys, N. N., Melville, C. P., 1982, A History of Persian Earthquakes. Cambridge University Press, Cambridge, 219 pp.

Asadian, O., 1993, Quadrangle map of Tabriz. Geological Survey of Iran, scale 1: 100000, 1 sheet.

Authemayou, C., Bellier, O., Chardon, D., Benedetti, L., Malekzade, Z., Claude, C. Angeletti, B., Shabanian, E., Abbassi, M. R., 2009, Quaternary slip-rates of the Kazerun and the Main Recent Faults: active strike-slip partitioning in the Zagros fold and-thrust belt, Geophys. J. Int. 178, 524–540.

Berberian, M., 1981, Active faulting and tectonics of Iran. In: Gupta, H. K. and Delany, F. M. (eds.), Zagros-Hindukush-Himalaya Geodynamic evolution, Am. Geophys. Union and Geol. Soc. Am. Geodyn. Ser. 3, 33-69.

Berberian, M., 1997, Seismic sources of the Transcaucasian historical earthquakes. In: Giardini, D., and Balassanian, S. (eds.), Historical and Prehistorical Earthquakes in the Caucasus. Kluwer Academic Publishing, Dordrecht, Netherlands 28, 233–311.

Berberian, M., 2014, Earthquakes and Coseismic Faulting on the Iranian Plateau: A Historical, Social and Physical Approach, Elsevier Series Development in Earth Surface Processes 17, Amsterdam, the Netherlands, 776 pp.

Berberian, F., Berberian, M., 1981, Tectono-Plotonic episodes in Iran. In: Gupta, H. K. and Delany, F. M. (eds.), Zagros-Hindukush-Himalaya Geodynamic evolution, Am. Geophys. Union and Geol. Soc. Am., Geodyn. Ser. 3, 5-32.

Berberian, M., Yeats, R. S., 1999, Patterns of historical earthquake rupture in the Iranian Plateau. Bull. Seism. Soc. Am. 89, 120–139.

Bottrill, A. D., Hunen, J. V., Allen, M. B., 2012, Insight into collision zone dynamics from topography: numerical modeling results and observations. Solid Earth 3, 387–399.

Bucci, D., Massa, B., Zuppetta, A., 2006, Relay ramps in active normal fault zones: A clue to the identifi cation of seismogenic sources (1688 Sannio earthquake, Italy). GSA Bulletin 118, 430-448.

Copley, A., Jackson, J., 2006, Active tectonics of the Turkish-Iranian Plateau, Tectonics 25, TC6006.

Copley, A., Faridi, M., Ghorashi, M., Hollingsworth, J., Jackson, J., Nazari, H., Oveisi, B., Talebian, M., 2014, The 2012 August 11 Ahar earthquakes: consequences for tectonics and earthquake hazard in the Turkish-Iranian Plateau. Geophys. J. Int. 196, 15–21.

DeMets, C., Gordon, R. G., Argus, D. F., Stein, S., 1990, Current plate motions. Geophys. J. Int. 101, 425- 478.

Dewey, J. F., Hempton, M. R., Kidd, W. S. F., Saroglu, F., Şengör, A. M. C., 1986, Shortening of continental lithosphere: the neotectonics of Eastern Anatolia- a young collision zone. In: Coward, M., and Ries, A. (eds.), Collision Tectonics. Special Publication of the Geological Society of London 19, 3–36.

Djamour, Y., Vernant, P., Nankali, H., Tavakoli, F., 2011, NW Iran-eastern Turkey present-day kinematics: results from the Iranian permanent GPS network. Earth planet. Sci. Lett. 307, 27–34.

Dooley, T. P., Schreurs, G., 2012, Analogue modelling of intraplate strike-slip tectonics: A review and new experimental results. Tectonophysics 574 –575, 1–71.

Faridi, M., Burg, J. P., Nazari, H., Talebian, M., Ghorashi, M., 2017, Active Faults Pattern and Interplay in the

Azarbaijan Region (NW Iran). Geotectonics 51, 428–437.

Forbes, R. J., 1964, Studies in Ancient Technology (Leiden, Netherlands: E.J. Brill). Vol. 1, 209 pp.

Gavillot, Y., Axen, G. J., Stockli, D. F., Horton, B. K., Fakhari, M. D., 2010, Timing of thrust activity in the High Zagros fold-thrust belt, Iran, from (U-Th)/he thermochronometry. Tectonics 29, 1–25.

Ghalamghash, J., Schmitt, A. K., Chaharlang, R., 2019, Age and compositional evolution of Sahand volcano in the context of post-collisional magmatism in northwestern Iran: Evidence for time-transgressive magmatism away from the collisional suture. Lithos 344-345, 265-279.

Goblot, H, 1979, Les Qanats: une Technique d'Acquisition de l'Eau (Paris, Mouton), 236 pp.

Gurbuz, A., Saroglu, F., 2018, Right-Lateral Strike-Slip Faulting and Related Basin Formations in the Turkish-Iranian Plateau. Developments in Structural Geology and Tectonics 3, 101-130.

Hempton, M. R., 1987, Constraints on Arabia plate motion and extensional history of the Red Sea. Tectonics 6, 687–705.

Hessami, K., Pantosti, D., Tabassi, H., Shabanian, E., Abbassi, M. R., Feghhi, K., Solaymani, S., 2003, Paleoearthquakes and slip rates of the North Tabriz Fault, NW Iran: preliminary results. Annals of Geophysics 46, 903-915.

Jackson, J. A., 1992, Partitioning of strike-slip and convergent motion between Eurasia and Arabia in eastern Turkey and the Caucasus. J. Geophys. Res. 97, 12471-12479.

Jackson, J. A., McKenzie. D. P., 1984, Active tectonics of the Alpine-Himalayan belt between western Turkey and Pakistan. Geophys. J. R. astr. Soc. 77, 185-264.

Jackson, J., Priestley, K., Allen M. B., Berberian, M., 2002, Active tectonics of the South Caspian Basin. Geophys. J. Int. 148, 214–245.

Kamiar, M., 1983, The Qanat system in Iran. Ekistics, 50, 467-472.

Khodabandeh, A. A., Amini Fazel, A., 1993, Quadrangle map of Osku. Geological Survey of Iran, scale 1: 100000, 1 sheet.

Khorrami, F., Vernant, Ph., Masson, F., Nilfouroushan, F., Mousavi, Z., Nankali, H., Saadat, S. A., Walpersdorf, A., Hosseini, S., Tavakoli, P., Aghamohammadi, A., Alijanzade, M., 2019, An up-to-date crustal deformation map of Iran using integrated campaign-mode and permanent GPS velocities. Geophys. J. Int. 217, 832–843.

McKenzie, D. P., 1972, Active tectonics of Mediterranean region. Geophys. J. R. astr. Soc. 30, 109-185.

McQuarrie, N., Stock, J. M., Verdel, C., Wernicke, B., 2003, Cenozoic evolution of Neotethys and implications for the causes of plate motions. Geophys. Res. Lett. 30, 1–4.

Melville, C. P., 1981, Historical Monuments and Earthquakes in Tabriz, Iran. Journal of the British Institute of Persian Studies 19, 159-177.

Mirzaei, N., Gao, M., Chen, Y. T., 1998, Seismic source regionalization for seismic zoning of Iran: major seismotectonic provinces. J. Earthquake prediction Research, 7, 465-495.

Mouthereau, F., 2011, Timing of uplift in the Zagros belt/Iranian Plateau and accommodation of late Cenozoic Arabia-Eurasia convergence. Geol. Mag. 148, 726–738.

Potts, D. T., 1990, From prehistory to the fall of the Achaemenid Empire, in The Arabian Gulf in Antiquity (Oxford, Clarendon Press). Vol. 1, 460 pp.

Reilinger, R., McClusky, S., Vernant, P., Lawrence, S., Ergintav, S., Cakmak, R., Ozener, H., Kadirov, F., Guliev, I.,

Stepanyan, R., Nadariya, M., Hahubia, G., Mahmoud, S., Sakr, K., Arrajehi, A., Paradissis, D., Al-Aydrus, A., Prilepin, M., Guseva, T., Evren, E., Dmitrotsa, A., Filikov, S. V., Gomez, F., Al-Ghazzi, R., Karam G., 2006, GPS constraints on continental deformation in the Africa-Arabia-Eurasia continental collision zone and implications for the dynamics of plate interactions. J. Geophys. Res. 111, B05411.

Ritz, J. F., Nazari, H., Ghassemi, A., Salamati, R., Shafei, A., Solaymani, S., Vernant, P., 2006, Active transtension inside central Alborz: a new insight into northern Iran-southern Caspian geodynamics. Geology 34, 477–480.

Rizza, M., Vernant, J., Ritz, F., Peyret, M., Nankali, H., Nazari, H., Djamour, Y., Salamati, R., Tavakoli, F., Chery, J., Mahan, S., Masson, F., 2013, Morphotectonic and geodetic evidence for a constant slip-rate over the last 45 kyr along the Tabriz fault (Iran). Geophys. J. Int. 199, 25–37.

Solaymani Azad, S., Nemati, M., Abbassi, M. R., Foroutan, M., Hessami, K., Dominguez, S., Bolourchi, M. J., Shahpasandzadeh, M., 2019, Active-couple indentation in geodynamics of NNW Iran: Evidence from synchronous left- and right-lateral co-linear seismogenic faults in western Alborz and Iranian Azarbaijan domains. Tectonophysics 754, 1–17.

Taghipour, K., Khatib, M. M., Heyhat, M., Shabanian, E., Vaezihir, A., 2018, Evidence for distributed active strike-slip faulting in NW Iran: The Maragheh and Salmas fault zones. Tectonophysics 742–743, 15–33.

Talebian, M., Jackson, J., 2002, Offset on the main recent fault of the NW Iran and implications on the late Cenozoic tectonics of the Arabia-Eurasia collision zone, Geophys. J. Int. 150, 422–439.

Trifonov, V. G., Kozhurin, A. I., 2010, Study of Active Faults: Theoretical and Applied Implications. Geotectonics 44, 510-528.

Valerio, E., Manzo, M., Casu, F., Convertito, V., De Luca, C., Manunta, M., Monterroso, F., Lanari, R., De Novellis, V., 2020, Seismogenic Source Model of the 2019, Mw 5.9, East-Azerbaijan Earthquake (NW Iran) through the Inversion of Sentinel-1 DInSAR Measurements. Remote Sensing 12, 1346.

Vernant et al., 2004, Contemporary Crustal Deformation and Plate Kinematics in Middle East Constrained by GPS Measurements in Iran and Northern Oman. Geophys. J. Int. 157, 381-398.

Vernant, P., Chéry, J., 2006, Mechanical modelling of oblique convergence in the Zagros, Iran, Geophys. J. Int. 165, 991–1002.

Vincent, S. J., Allen, M. B., Ismail-Zadeh, A. D., Flecker, R., Foland, K. A., Simmons, M. D., 2005, Insights from the Talysh of Azerbaijan into the Paleogene evolution of the South Caspian region. Bull. Geol. Soc. Am. 117, 1513–1533.

Walker, R. T., Bergman, E. A., Elliott, J. R., Fielding, E. J., Ghods, A. R., Ghoraishi, M., Jackson, J., Nazari, H., Nemati, M., Oveisi, B., Talebian, M., Walters, R. J., 2013, The 2010–2011 South Rigan (Baluchestan) earthquake sequence and its implications for distributed deformation and earthquake hazard in southeast Iran. Geophys. J. Int. 93, 349–374.

Yazdi, P., Santoyo, M. A., Gaspar-Escribano, J. M., 2018, Analysis of the 2012 Ahar- Varzeghan (Iran) seismic sequence: Insights from statistical and stress transfer modeling. Global and Planetary Change 161, 121–131.

Yeats, R., 2012, Active Faults of the World. Cambridge University Press, 621 pp.